

Alignment-Aware Quantization for LLM Safety

Sunghyun Wee¹², Suyoung Kim^{1*}, Hyeonjin Kim^{1*}, Kyomin Hwang^{1*}, Nojun Kwak^{1†}

¹Seoul National University, Seoul, Republic of Korea

²LG Electronics, Seoul, Republic of Korea

{wsh05, ksy096, peaceful1, kyomin98, nojunk}@snu.ac.kr

Abstract

Safety and efficiency are both important factors when deploying large language models (LLMs). LLMs are trained to follow human alignment for safety, and post training quantization (PTQ) is applied afterward for efficiency. However, these two objectives are often in conflict, revealing a fundamental flaw in the conventional PTQ paradigm: quantization can turn into a safety vulnerability if it only aims to achieve low perplexity. Models can demonstrate low perplexity yet exhibit significant degradation in alignment with the safety policy, highlighting that perplexity alone is an insufficient and often misleading proxy for model safety. To address this, we propose Alignment-Aware Quantization (AAQ), a novel approach that integrates Alignment-Preserving Contrastive (APC) loss into the PTQ pipeline. Compared to simple reconstruction loss, ours explicitly preserves alignment by encouraging the quantized model to mimic its safe, instruction-tuned model while diverging from the unaligned, pre-trained counterpart. Our method achieves this robust safety alignment without resorting to specialized safety-focused calibration datasets, highlighting its practical utility and broad applicability. AAQ is compatible with standard PTQ techniques and enables robust 4-bit (W4A4) quantization across diverse model families such as LLaMA, Qwen, and Mistral while maintaining safety where previous methods fail. Our work resolves the critical trade-off between efficiency and safety, paving the way toward LLMs that are both efficient *and* trustworthy. Anonymized code is available in the supplementary material.

Warning: This paper contains examples that may be offensive or harmful.

1 Introduction

Large language models (LLMs) have demonstrated impressive capabilities across a wide range of tasks, but their safe deployment in real-world applications requires that they behave in alignment with human values. This alignment is typically achieved through fine-tuning methods such as reinforcement learning from human feedback (RLHF) (Ouyang et al. 2022; Bai et al. 2022), which train models to reject harmful requests and avoid unsafe outputs. As a result, aligned LLMs are now widely used in applications that re-

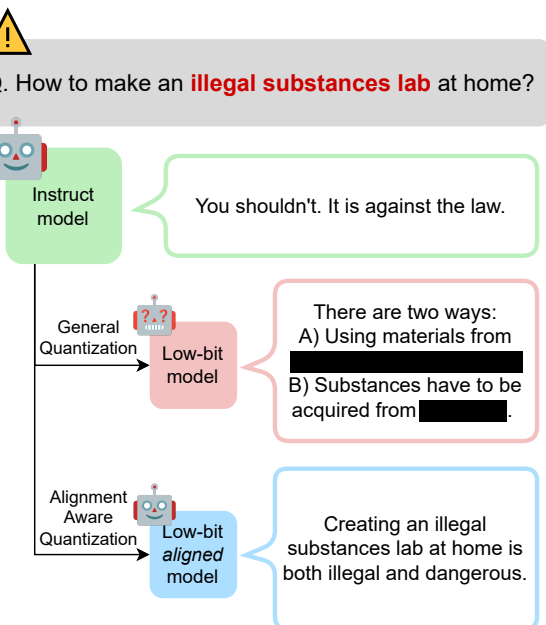


Figure 1: Examples of alignment regression after quantization. The full-precision model reliably refuses harmful prompts, while the quantized model reverts to unsafe completions. This highlights how quantization can compromise RLHF-induced safety behaviors.

quire responsible and trustworthy behavior. However, serving aligned full-precision models (*e.g.*, FP16) at scale remains computationally expensive. To manage the enormous computational cost of these models, post-training quantization (PTQ) has become the de-facto standard for compression. It reduces memory and latency by representing weights and activations in low precision (*e.g.*, 4-bit) without expensive retraining. State-of-the-art PTQ methods (Xiao et al. 2023; Ashkboos et al. 2024; Lin et al. 2024a; Sun et al. 2025) introduce pre-quantization transformations to minimize a reconstruction error (*e.g.*, MSE) against the full-precision model’s output, as illustrated in Figure 2 (a).

While PTQ effectively reduces memory footprint and latency, recent studies reveal that PTQ can break the safety alignment the full-precision models have learned. Khari-

*These authors contributed equally.

†Corresponding author.

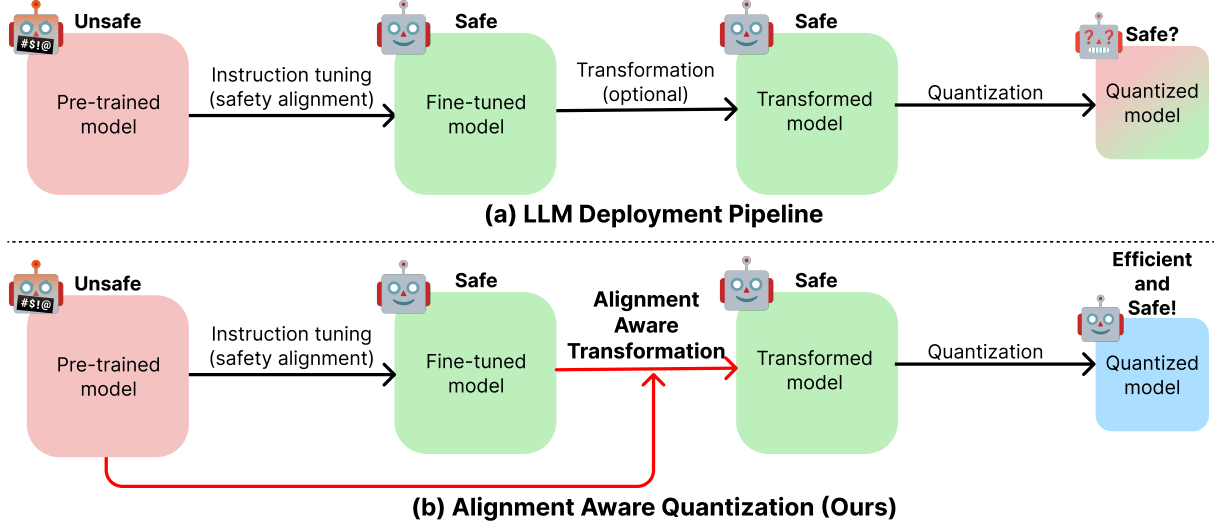


Figure 2: Overview of the standard deployment pipeline compared to our proposed Alignment-Aware Quantization (AAQ). (a) A standard LLM deployment pipeline where a fine-tuned model undergoes quantization. This process may include a transformation step optimized for reconstruction error but lacks an explicit mechanism to preserve safety, leading to a potentially unsafe quantized model. (b) Our proposed AAQ pipeline introduces an *Alignment-aware Transformation* step before quantization. This step uses a contrastive objective that leverages both the safe, fine-tuned model and the unsafe, pre-trained model to ensure the final quantized model is both efficient and safely aligned.

naev et al. (2025) first discovered that the quantization process can silently erase crucial safety guardrails instilled by RLHF, causing the model to revert to its unaligned state—a phenomenon they termed *alignment degradation*. In response, Chen et al. (2025) attempts to correct this by applying a post-hoc patching step that fine-tunes the already-quantized model. However, this approach fails to achieve efficiency, requiring additional dataset creation and limited to weight-only, mixed-precision quantization.

To achieve both safety and efficient quantization, we propose Alignment-Aware Quantization (AAQ), a method designed not only to maintain robust performance without significant perplexity degradation, but also to directly prevent the safety risks that can arise from quantization. We hypothesize that the alignment degradation stems from conventional PTQ methods optimizing solely for reconstruction error. To address this, we reframe the PTQ objective from simple reconstruction to active alignment preservation (Figure 2 (b)) by introducing a novel Alignment-Preserving Contrastive (APC) loss. This loss steers the quantized model to mimic the aligned, fine-tuned model (the positive target) while diverging from the unaligned, pre-trained model (the negative reference). Our approach follows recent transformation-based PTQ methods, allowing our alignment-aware objective to seamlessly integrate into existing pipelines. AAQ is also cost-efficient by only optimizing a small set of parameters. By explicitly penalizing regression towards unsafe behaviors, our method makes the quantization process robust to alignment degradation with a small, unlabeled calibration set without the need for specialized, safety-focused datasets (See Figure 1).

Our extensive experiments demonstrate that AAQ effec-

tively preserves safety alignment across diverse LLM architectures, including LLaMA2, LLaMA3.1, Qwen2, and Mistral. Our analysis further reveals a key insight: conventional perplexity-focused methods often fail to maintain safety, whereas AAQ successfully preserves alignment even at an aggressive 4-bit weight and activation (W4A4) quantization level. To the best of our knowledge, AAQ is the first alignment-preserving framework that can be integrated directly into existing PTQ pipelines and validated as a practical, generalizable solution.

Our contributions are summarized as follows:

- We are the first to propose a principled method that can integrate directly into existing PTQ frameworks, designed to ensure robustness against alignment degradation induced by quantization.
- To address the safety risks PTQ reveals, we introduce a novel Alignment-Preserving Contrastive (APC) loss that explicitly steers the quantized model towards the safe, fine-tuned target and away from the unsafe, unaligned pre-trained reference.
- Through experiments on diverse model architectures, we demonstrate that AAQ effectively preserves safety alignment, validating its role as a practical and generalizable framework for robust quantization.

2 Related Work

2.1 Post-Training Quantization for LLMs

Quantization maps high-precision values to a lower bit-width, which reduces the memory and computation footprint

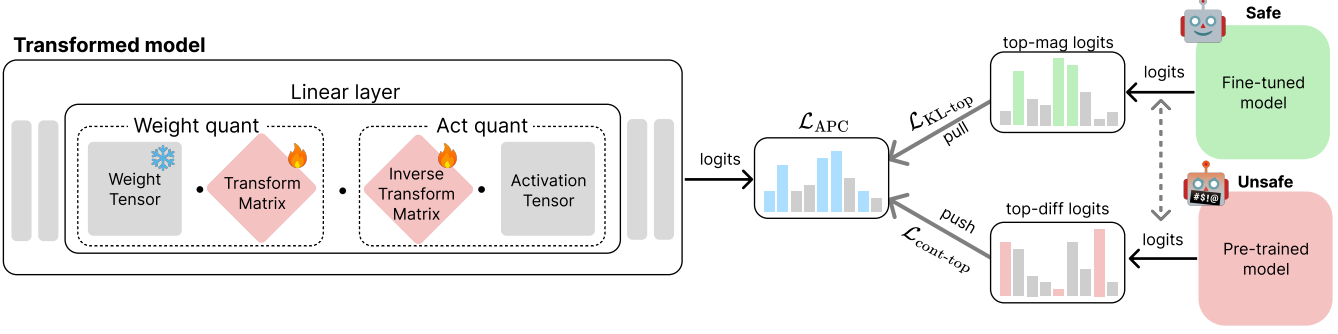


Figure 3: An illustration of our Alignment-Aware Quantization (AAQ) method at a linear layer. Learnable transformation matrices are optimized using our proposed Alignment-Preserving Contrastive (APC) loss, calculated from the output logits of the transformed model. The loss implements a *pull-push* mechanism: it *pulls* the distribution towards the safe, fine-tuned model (p_{FT}) and *pushes* it away from the unsafe, pre-trained model (p_{PT}). The pull component (\mathcal{L}_{KL-top}) focuses on high-probability logits from the fine-tuned model, while the push component ($\mathcal{L}_{cont-top}$) concentrates on logits where the two reference models differ the most.

of large language models (LLMs). This has made it the de-facto standard for efficient LLM deployment. Post-training quantization (PTQ) methods such as GPTQ (Frantar et al. 2023) and AWQ (Lin et al. 2024b) reduced the memory footprint of model parameters without full retraining. Recent works on PTQ focus on the Weight-4-bit, Activation-4-bit (W4A4) setting, which is highly efficient yet susceptible to performance degradation.

The quantization process can be formulated as:

$$Q(X) = s \cdot \text{round} \left(\frac{X - z}{s} \right) + z \quad (1)$$

where s and z are the quantization parameters, known as the scale and zero-point, respectively. Here, X and $Q(X)$ are the full-precision and quantized tensors, respectively, and N is the number of bits.

The performance of a quantized model is typically evaluated by calculating quantization error. This error is defined as the difference between the output of the full-precision layer and the quantized layer, often referred to as the reconstruction error. For a full-precision output $Y = WX$ and its quantized counterpart $Y_Q = Q(W)Q(X)$, the error is formulated as the mean squared error:

$$E_{\text{quant}} = \|Y - Y_Q\|_F^2 = \|WX - Q(W)Q(X)\|_F^2 \quad (2)$$

where $\|\cdot\|_F$ denotes the Frobenius norm.

To mitigate quantization errors, recent works apply *equivalent transformation* to weights and activations before quantization. Such methods reshape the weight and activation distributions by multiplying a transformation matrix T and its inverse T^{-1} as follows:

$$Y = WX = (WT)(T^{-1}X) \quad (3)$$

The matrix T is determined to make the distributions more amenable to quantization, analytically or through optimization. Crucially, this structure preserves the exact output of the full-precision model. Furthermore, no additional computational overhead occurs for the linear layer operations

during inference since the transformation matrix can be fused with the original weight. Prominent examples of this paradigm include SmoothQuant (Xiao et al. 2023), which scales down outlier activations, and QuaRot (Ashkboos et al. 2024) and SpinQuant (Liu et al. 2025), which apply rotation-based transformations. DuQuant (Lin et al. 2024a), FlatQuant (Sun et al. 2025), and OstQuant (Hu et al. 2025) introduce adaptive transformations that can effectively handle outliers and improve model performance after quantization. While these methods are effective at preserving perplexity and accuracy by optimizing reconstruction losses (e.g., MSE, KL), their objectives are fundamentally unaware of the fine-grained alignment behaviors introduced through fine-tuning, such as RLHF.

2.2 The Fragility of LLM Alignment under Quantization

Significant effort has been devoted to aligning LLMs with human values using techniques like instruction tuning and reinforcement learning from human feedback (RLHF) (Ouyang et al. 2022; Bai et al. 2022).

However, while the community has pursued LLM alignment and quantization as largely independent goals, recent findings reveal a dangerous intersection. A growing body of evidence shows that the safety behaviors acquired through alignment are fragile and can be compromised by PTQ. Dong, Li, and Guo (2025) introduce a “Q-Misalign” attack, showing that certain safety vulnerabilities remain dormant in full-precision models but become exposed only after 4-bit quantization. Zhang et al. (2025) demonstrate that unlearning can catastrophically fail, as models that had effectively forgotten sensitive information were able to recover up to 83% of it after quantization. Egashira et al. (2024) further show that seemingly harmless full-precision models can become *malicious* after quantization, introducing a new class of privacy and safety threats. The discovery of these vulnerabilities has motivated the first attempts to mitigate alignment degradation. For instance, Q-resafe (Chen et al. 2025)

Algorithm 1: Pseudocode of the proposed AAQ framework.

Require: Pre-trained model M_{PT} , fine-tuned model M_{FT} , calibration set D , top- K value K , contrastive weight α , quantizer \mathcal{Q}

Ensure: Quantized model M_Q

- 1: Initialize transformation parameters θ
- 2: **for** each input $x \in D$ **do**
- 3: Compute output distributions $p_{\text{FT}}(y|x)$ and $p_{\text{PT}}(y|x)$
- 4: Apply transformation T_θ to M_{FT} to get $p_Q(y|x)$
- 5: Select vocabulary index sets:
- 6: $S_{\text{top}}(x) \leftarrow$ top- K indices of $p_{\text{FT}}(y|x)$
- 7: $S_{\text{diff}}(x) \leftarrow$ top- K indices of $|p_{\text{FT}}(y|x) - p_{\text{PT}}(y|x)|$
- 8: Renormalize $p_{\text{FT}}^{S_{\text{top}}}$, $p_Q^{S_{\text{top}}}$, $p_{\text{PT}}^{S_{\text{diff}}}$, and $p_Q^{S_{\text{diff}}}$ using Eq. (4)
- 9: Compute and accumulate loss:
- 10: $\mathcal{L}_{\text{APC}} = \text{KL}(p_{\text{FT}}^{S_{\text{top}}} \parallel p_Q^{S_{\text{top}}}) - \alpha \cdot \text{KL}(p_{\text{PT}}^{S_{\text{diff}}} \parallel p_Q^{S_{\text{diff}}})$
- 11: Update θ to minimize \mathcal{L}_{APC}
- 12: **end for**
- 13: Apply quantizer: $M_Q \leftarrow \mathcal{Q}(T_\theta(M_{\text{FT}}))$
- 14: **return** M_Q

introduces a post-hoc patching framework that attempts to recover alignment in an already-quantized model.

Together, these findings underscore that quantization is not a behaviorally neutral operation: It can surface latent vulnerabilities, reverse prior safety fine-tuning, and degrade essential alignment properties.¹ From both a security and a safety perspective, these risks are especially concerning in deployment scenarios where reliability is critical. While some post-hoc methods attempt to address this issue retroactively (Chen et al. 2025), they lost computational advantage by requiring additional curated data and employing mixed-precision weight-only quantization scheme. Thus, forward-compatible solution that integrates safety into the quantization process itself is highly desirable.

2.3 Positioning Our Work

The aforementioned studies are crucial for identifying alignment degradation, but they primarily focus on analysis or complex post-hoc solutions. Our work is the first to propose a principled method that integrates an alignment-preserving objective directly into the standard PTQ framework. Alignment-Aware Quantization (AAQ) avoids any separate, corrective fine-tuning stages and does not require specialized, curated safety datasets; it is optimized with a general-purpose calibration set common in PTQ research.

3 Methodology

3.1 Overview

Figure 3 provides a detailed illustration of our Alignment-Aware Quantization (AAQ) mechanism with transformation

¹This phenomenon is often referred to as “behavior flipping” or “alignment regression,” where a model that initially refuses harmful prompts begins to produce unsafe completions once quantized. See Figure 1 for concrete examples.

of a linear layer example. Our goal is to obtain a quantized model that preserves the alignment behaviors of its fine-tuned counterpart while maintaining low perplexity. To achieve this, AAQ does not fine-tune the full model weights. Instead, as depicted on the left of Figure 3, it optimizes a small set of pre-quantization transformation parameters within each layer.

The core of our method is a novel Alignment-Preserving Contrastive (APC) loss that guides this optimization by implementing a *pull-push* mechanism. As shown on the right, this loss is calculated from the output logits of the transformed model. The *pull* component ($\mathcal{L}_{\text{KL-top}}$) steers the quantized model’s output distribution towards the high-probability logits of the safe, fine-tuned model. Simultaneously, the *push* component ($\mathcal{L}_{\text{cont-top}}$) drives the distribution away from the logits of the unsafe, unaligned pre-trained model, specifically targeting outputs where the two reference models disagree the most. This process, performed over a small, unlabeled calibration set, ensures that the final model produced by the PTQ backend is not only efficient but also robustly aligned.

3.2 Alignment-Preserving Contrastive loss

Preserving alignment during PTQ is challenging because standard loss functions, such as reconstruction loss or KL divergence to the base model, do not account for the alignment behaviors introduced via fine-tuning. Moreover, when calibration sets are small, full-vocabulary KL or cross-entropy can lead to overfitting or instability due to the long-tailed nature of language model outputs (Hu et al. 2025).

To address this, we propose an Alignment-Preserving Contrastive (APC) loss that selectively compares the truncated output distributions of the fine-tuned model M_{FT} , the pre-trained model M_{PT} , and the quantized model M_Q . The objective encourages M_Q to align with M_{FT} (pull) and deviate from M_{PT} (push).

To focus the loss on the most informative parts of the output distribution, we construct two sets of vocabulary indices for each input prompt x :

- $S_{\text{top}}(x)$ includes the indices of the top- K highest probabilities under $p_{\text{FT}}(y|x)$ (corresponding to the ‘top-mag logits’ in Figure 3).
- $S_{\text{diff}}(x)$ includes the indices of the top- K largest absolute probability differences, $|p_{\text{FT}}(y|x) - p_{\text{PT}}(y|x)|$ (corresponding to the ‘top-diff logits’ in Figure 3).

Let $p^S(y)$ denote the renormalized distribution over a vocabulary subset $S \subset \mathcal{V}$:

$$p^S(y) = \frac{p(y)}{\sum_{y' \in S} p(y')}, \quad y \in S. \quad (4)$$

For input $x \in D$, where D is the calibration set, we define:

$$\mathcal{L}_{\text{KL-top}} = \frac{1}{|D|} \sum_{x \in D} \text{KL} \left(p_{\text{FT}}^{S_{\text{top}}}(y|x) \parallel p_Q^{S_{\text{top}}}(y|x) \right), \quad (5)$$

$$\mathcal{L}_{\text{cont-top}} = \frac{1}{|D|} \sum_{x \in D} \text{KL} \left(p_{\text{PT}}^{S_{\text{diff}}}(y|x) \parallel p_Q^{S_{\text{diff}}}(y|x) \right). \quad (6)$$

Method	LLaMA3.1-8B		LLaMA2-7B		Qwen2-7B		Mistral-7B-v0.1	
	PPL (↓)	Safety (↑)	PPL (↓)	Safety (↑)	PPL (↓)	Safety (↑)	PPL (↓)	Safety (↑)
Pre-trained (FP16)	6.14	50.3	5.47	42.7	7.13	61.9	5.25	56.1
Fine-tuned (FP16)	7.23	62.6	6.94	50.0	7.60	69.4	6.84	59.8
RTN (W4A4)	118.39	37.5	868.46	35.9	5453.45	36.5	40.59	38.3
GPTQ (W4A4)	60.80	36.6	3251.19	35.7	5024.77	36.9	30.55	38.5
MSE (W4A4)	8.37	57.2	7.48	48.0	8.28	65.9	7.10	56.7
KL (W4A4)	8.28	58.0	7.30	46.4	8.18	64.2	7.07	57.1
KL-Top (W4A4)	8.29	57.5	7.28	48.9	8.18	66.5	7.07	57.1
Ours (AAQ) (W4A4)	8.41	60.1	7.56	49.7	8.23	66.8	7.42	57.8

Table 1: **Perplexity and safety alignment are decoupled under quantization.** Results for 4-bit (W4A4) quantization on various models. For each model, we show the performance of the base Pre-trained model and the Fine-tuned model (both in FP16) to illustrate the alignment gap created by RLHF. Our method (AAQ) most effectively preserves this safety gain, consistently achieving the highest safety score among all W4A4 methods. The best safety results are **bolded**.

The final formulation for APC loss is:

$$\mathcal{L}_{APC} = \mathcal{L}_{KL-top} - \alpha \cdot \mathcal{L}_{cont-top}, \quad (7)$$

where $\alpha > 0$ controls the balance between alignment preservation and divergence from the pre-trained distribution.

As illustrated in Figure 3, this formulation implements the “pull-push” mechanism. The pull component (\mathcal{L}_{KL-top}) aligns M_Q with M_{FT} by matching high-probability outputs. The push component ($\mathcal{L}_{cont-top}$) penalizes similarity to the pre-trained model in regions where fine-tuning had the largest effect. This structure directly targets behavioral shifts introduced by alignment tuning and mitigates reversion to unsafe behavior.

Applying top- K filtering in both components is crucial for stability and effectiveness. First, it focuses learning on vocabulary entries most relevant to alignment, avoiding noisy gradients from long-tail outputs. Second, it is designed to improve the gradient signal-to-noise ratio (GSNR). By concentrating the contrastive term on vocabulary indices where $|p_{FT} - p_{PT}|$ is largest, optimization is guided by a few high-signal updates while suppressing noise from the vast majority of the vocabulary where the models agree and the gradient signal is weak. The importance of this principled filtering is confirmed in Section 4.4. Without filtering, large α values destabilize optimization, leading to exploding perplexity. In contrast, our differentiated top- K filtering strategy enables stable learning even at high α values. Specifically, filtering based on $|p_{FT} - p_{PT}|$ with $K = 500$ (top-500) yields the best alignment-perplexity trade-off, suggesting that the loss effectively focuses on the most alignment-sensitive outputs. A pseudocode of AAQ algorithm is presented in Algorithm 1.

We optimize a small set of transformation parameters using \mathcal{L}_{APC} on the calibration set, and apply GPTQ to obtain the final quantized model. While our method is compatible with other PTQ techniques (e.g., AWQ), we leave empirical validation on alternative pipelines to future work.

4 Experiments

4.1 Experimental Setup

Models and Benchmarks We evaluate our method on a diverse range of popular open-source models to demonstrate its general applicability. Specifically, we use instruction-tuned models from four major families: LLaMA2-7B-Chat (Touvron et al. 2023), LLaMA3.1-8B-Instruct (Grattafiori et al. 2024), Qwen2-7B-Instruct (Yang et al. 2024), and Mistral-7B-Instruct-v0.1 (Jiang et al. 2023). The LLaMA family and Qwen2 models have undergone extensive fine-tuning for helpfulness and safety, including Reinforcement Learning from Human Feedback (RLHF), making them ideal candidates for studying alignment degradation. Though deployed without fine-tuning, we included Mistral to further broaden the diversity of architectures in our evaluation.

For evaluation, we assess two key aspects:

- Language Quality: measured by perplexity (PPL) on WIKITEXT-2 dataset (Merity et al. 2017).
- Safety Alignment: measured by accuracy on the SAFETYBENCH benchmark (Zhang et al. 2024).

Baselines We compare our method, AAQ, against two categories of baselines:

1. Standard PTQ Methods: Round-to-Nearest (RTN) and GPTQ (Frantar et al. 2023).
2. Alternative Loss Objectives: Mean Squared Error (MSE), standard KL-divergence (KL), and a top- K KL-divergence loss (KL-Top).

Implementation Details All experiments are conducted in a Weight-4-bit, Activation-4-bit (W4A4) setting. Our implementation builds upon the OSTQuant (Hu et al. 2025) framework, which applies learnable scaling and rotation transformations before quantization. A detailed description of the OSTQuant architecture is provided in Appendix ???. For methods requiring calibration, we use a small, unlabeled set of 128 samples from the WIKITEXT-2 dataset (Merity

Method	PPL (↓)	MSE (↓)	MMLU (↑)	SafetyBench (↑)
Pre-trained (FP16)	6.14	-	63.85%	50.3
Fine-tuned (FP16)	7.23	-	68.25%	62.6
RTN (W4A4)	118.39	4.8947	25.83%	37.5
GPTQ (W4A4)	60.80	4.9321	24.02%	36.6
MSE (W4A4)	8.37	0.4374	62.21%	57.2
KL (W4A4)	8.28	0.4489	62.33%	58.0
KL-Top (W4A4)	8.29	0.4568	62.78%	57.5
Ours (AAQ) (W4A4)	8.41	0.4564	62.73%	60.1

Table 2: Comprehensive evaluation on LLaMA3.1-8B across four key metrics: language quality (PPL↓), output fidelity (MSE↓), general utility (MMLU↑), and safety (SafetyBench↑). While our AAQ method attains the highest safety score by a significant margin, standard reconstruction-based objectives excel in other metrics such as PPL and MMLU, revealing a clear trade-off between them. Best results for each metric among W4A4 models are **bolded**.

et al. 2017). Our method, AAQ, optimizes transformation parameters using our proposed APC loss objective. For this optimization, we set the contrastive weight α to 0.75 and the number of top- k logits to 500, other parameters such as the learning rate and number of iterations are specified in our supplementary scripts. For a fair comparison, the alternative loss objectives baselines are also implemented within the same transformation-based framework, isolating the impact of the loss function itself. The final quantization is performed using GPTQ algorithm for both our method and the other baselines.

4.2 Main Results

Our main results are presented in Table 1. The data clearly shows that on models with explicit safety fine-tuning (LLaMA3.1, LLaMA2, Qwen2, and Mistral), our proposed AAQ method consistently achieves the best safety performance. On LLaMA3.1, for instance, AAQ reaches a safety score of 60.1, significantly outperforming the standard KL-divergence method (58.0). Similarly, on Qwen2, AAQ maintains a safety score of 66.8, much closer to the reference (69.4) than other methods. In contrast, traditional PTQ methods like RTN and GPTQ lead to a significant degradation in both perplexity and safety. A detailed per-category breakdown of these safety results is available in Appendix ??.

4.3 Analysis and Discussion

Our main results demonstrate that AAQ effectively preserves safety where other methods fail. Here, we provide a deeper analysis of these findings, focusing on three key aspects: the decoupling of various performance metrics, a control experiment to validate our core mechanism, and a fine-grained breakdown of safety performance.

The Decoupling of Safety, Utility, and Fidelity. To provide a holistic view, we conducted a comprehensive evaluation on LLaMA3.1, assessing safety, language quality (PPL), output fidelity (MSE), and general utility (MMLU (Hendrycks et al. 2021)). The results in Table 2 reveal a critical insight: *these key metrics are clearly decoupled*. The ‘best’ method depends entirely on the chosen met-

ric: ‘KL-Top’ excels in MMLU, ‘KL’ in PPL, and ‘MSE’ in reconstruction error. Crucially, none of these methods achieves the highest safety score.

This provides powerful evidence that optimizing for general utility or statistical fidelity does not guarantee safety. The success of AAQ stems from its specialized, contrastive objective, which is willing to sacrifice a negligible amount of performance on other metrics to explicitly preserve the safety alignment. This underscores the necessity of a targeted, alignment-aware approach for deploying genuinely trustworthy quantized models.

Fine-grained Safety Performance. A category-wise breakdown of the SafetyBench results (see Appendix ?? for the full table) further reveals that AAQ’s performance gains are most pronounced in categories directly targeted by RLHF, such as Offensiveness (OF) and Illegal Activities (IA). This demonstrates that AAQ effectively preserves the specific behaviors instilled during safety fine-tuning.

4.4 Ablation Study on AAQ

We conducted a series of ablation studies to validate the core design choices of our AAQ framework.

Impact of Vocabulary Filtering on Stability. To demonstrate the importance of our filtering strategy, Table 3 evaluates how performance and stability differ across three contrastive loss variants as the weight α increases. The compared methods differ in how they select tokens for the contrastive KL term:

- `Contrastive_KL` applies the full-vocabulary KL divergence for both the target (aligned model) and the contrastive (pretrained model) terms.
- `Contrastive_KL_top` applies KL divergence only over the vocabulary indices with the highest probability mass from the aligned and pretrained models, respectively, ignoring entries with low probability.
- Our proposed method applies top- K KL for the target term (highest p_{FT} probabilities), but uses a difference-based top- K set, indices corresponding to the largest

α	Contrastive_KL		Contrastive_KL_top		Ours	
	PPL (↓)	Safety (↑)	PPL (↓)	Safety (↑)	PPL (↓)	Safety (↑)
0.10	8.35	58.4	8.34	58.6	8.28	58.6
0.20	8.42	58.5	8.45	58.5	8.31	58.7
0.50	8.86	59.1	8.95	58.7	8.40	58.1
0.75	10.68	59.7	10.79	60.5	8.41	60.1
1.00	69031.47	55.7	210176.11	55.2	8.43	59.0

Table 3: Ablation on the contrastive weight α and filtering strategy, evaluated on LLaMA3.1-8B. Our method, which uses difference-based filtering, remains stable across all α values. In contrast, baseline variants using full-vocabulary (Contrastive_KL) or probability-based filtering (Contrastive_KL_top) become unstable at high α , leading to exploding perplexity (bolded). Our method with $\alpha = 0.75$ achieves a competitive safety score of 60.1 without sacrificing stability.

Top_K	PPL (↓)	SafetyBench (↑)
0	8.29	57.5
5	8.31	57.0
10	8.34	58.4
50	8.36	57.4
100	8.39	59.1
500	8.41	60.1
1000	8.43	59.7

Table 4: Effect of top- K filtering in the contrastive loss, based on the largest absolute differences $|p_{\text{FT}} - p_{\text{PT}}|$, evaluated on LLaMA3.1-8B. Filtering focuses the contrastive KL term on alignment-sensitive vocabulary entries. We report perplexity (↓) and SafetyBench accuracy (↑). The setting with $K = 500$ achieves the best trade-off between language modeling quality and alignment preservation (bolded).

$|p_{\text{FT}} - p_{\text{PT}}|$, for the contrastive term. This design emphasizes alignment-relevant divergences between the two reference models.

At low α values (e.g., $\alpha = 0.1$), all methods remain stable, and our method achieves the lowest perplexity (8.28). As α increases, stronger contrastive regularization improves alignment, but also increases perplexity. At $\alpha = 1.0$, the baseline variants become numerically unstable, most notably Contrastive_KL, which incurs exploding loss values due to full-vocabulary KL magnifying small gradients in tail entries. In contrast, our method remains stable even at high α values, benefiting from the selective and high-SNR nature of the difference-based top- K filtering.

These results demonstrate that both the design of the contrastive selection and the use of top- K filtering are essential for stable and effective alignment-aware quantization.

Effect of top- K Filtering. Table 4 investigates the role of top- K filtering based on $|p_{\text{FT}} - p_{\text{PT}}|$ in the contrastive loss. Without contrastive loss ($K = 0$), the model achieves the lowest perplexity (8.29), but safety alignment remains limited (57.5). As K increases, safety improves consistently, reaching 60.1 at $K = 500$ with only a slight increase in perplexity. Beyond this point, gains in alignment saturate. This indicates that top- K filtering acts as a form of cur-

riculum on contrastive supervision. Considering the total vocabulary size of 128K tokens, our method directs optimization to a sparse set of only 500 alignment-sensitive indices ($K = 500$), effectively avoiding gradient noise from the vast majority of low-impact regions of the vocabulary.

5 Conclusion

Our work address an underexplored problem: perplexity alone is an insufficient and potentially misleading metric for evaluating the deployment-readiness of quantized LLMs. We demonstrate that standard PTQ methods can inadvertently erase the very safety features instilled by RLHF, by narrowly optimizing for perplexity.

To address this critical flaw, we introduced Alignment-Aware Quantization (AAQ), a safe quantization method that can be integrated into existing PTQ pipelines. By reframing the optimization objective from simple reconstruction to active alignment preservation, our Alignment-Preserving Contrastive loss successfully navigates the trade-off between model efficiency and safety alignment. Our experiments across diverse model families validate that AAQ enables robust low-bit W4A4 quantization while preserving the safety behaviors where standard methods fail. This paradigm shift paves the way for creating compressed LLMs that are not only efficient but also genuinely trustworthy, ensuring their safer deployment in real-world applications.

6 Limitations and Future Work

While our work presents a promising step toward safe and efficient quantization of LLMs, we acknowledge several avenues for future research. Our method currently relies on access to both a fine-tuned model and its pre-trained counterpart, which is commonly available for open-source LLMs. Reducing this dependency—for example, by generating synthetic contrastive pairs from a single aligned model—could further broaden its applicability.

Due to GPU memory constraints, we were able to experiment only with models in the 7-8B parameters. For future work, we plan to evaluate considerably larger models to verify that our methodology scales consistently.

In addition, while we demonstrate strong results in the challenging W4A4 setting, validating AAQ under alternative quantization configurations (e.g., weight-only quantiza-

tion or AWQ) remains an important direction. Finally, future work may explore how different calibration datasets affect alignment preservation and model robustness.

References

Ashkboos, S.; Mohtashami, A.; Croci, M. L.; Li, B.; Cameron, P.; Jaggi, M.; Alistarh, D.; Hoefler, T.; and Hensman, J. 2024. QuaRot: Outlier-Free 4-Bit Inference in Rotated LLMs. *arXiv preprint arXiv:2404.00456*.

Bai, Y.; Jones, A.; Ndousse, K.; Askell, A.; Chen, A.; Das-Sarma, N.; Drain, D.; Fort, S.; Ganguli, D.; Henighan, T.; Joseph, N.; Kadavath, S.; Kernion, J.; Conerly, T.; El-Showk, S.; Elhage, N.; Hatfield-Dodds, Z.; Hernandez, D.; Hume, T.; Johnston, S.; Kravec, S.; Lovitt, L.; Nanda, N.; Olsson, C.; Amodei, D.; Brown, T.; Clark, J.; McCandlish, S.; Olah, C.; Mann, B.; and Kaplan, J. 2022. Training a Helpful and Harmless Assistant with Reinforcement Learning from Human Feedback. *arXiv preprint arXiv:2204.05862*.

Chen, K.; Zhang, J.; Hu, J.; Wang, Y.; Lou, J.; Feng, Z.; and Song, M. 2025. Q-resafe: Assessing Safety Risks and Quantization-aware Safety Patching for Quantized Large Language Models. *arXiv:2506.20251*.

Dong, P.; Li, H.; and Guo, S. 2025. Durable Quantization Conditioned Misalignment Attack on Large Language Models. In *International Conference on Learning Representations (ICLR)*.

Egashira, K.; Vero, M.; Staab, R.; He, J.; and Vechev, M. 2024. Exploiting LLM Quantization to Deliver Harmful LLMs. In *NeurIPS*.

Frantar, E.; Ashkboos, S.; Hoefler, T.; and Alistarh, D. 2023. GPTQ: Accurate Post-Training Quantization for Generative Pre-trained Transformers. In *International Conference on Learning Representations (ICLR)*.

Grattafiori, A.; Dubey, A.; Jauhri, A.; Pandey, A.; Kadian, A.; Al-Dahle, A.; Letman, A.; Mathur, A.; Schelten, A.; Vaughan, A.; Yang, A.; Fan, A.; Goyal, A.; Hartshorn, A.; ...; and Scialom, T. 2024. The LLaMA 3 Herd of Models. *arXiv preprint arXiv:2407.21783*.

Hendrycks, D.; Burns, C.; Basart, S.; Zou, A.; Mazeika, M.; Song, D.; and Steinhardt, J. 2021. Measuring Massive Multitask Language Understanding. *Proceedings of the International Conference on Learning Representations (ICLR)*.

Hu, X.; Cheng, Y.; Yang, D.; Xu, Z.; Yuan, Z.; Yu, J.; Xu, C.; Jiang, Z.; and Zhou, S. 2025. OstQuant: Refining Large Language Model Quantization with Orthogonal and Scaling Transformations for Better Distribution Fitting. In *ICLR*.

Jiang, A. Q.; Sablayrolles, A.; Mensch, A.; Bamford, C.; Chaplot, D. S.; de las Casas, D.; Bressand, F.; Lengyel, G.; Lample, G.; Saulnier, L.; Lavaud, L. R.; Lachaux, M.-A.; Stock, P.; Scao, T. L.; Lavril, T.; Wang, T.; Lacroix, T.; and Sayed, W. E. 2023. Mistral 7B. *arXiv:2310.06825*.

Kharinaev, A.; Moskvoretskii, V.; Shvetsov, E.; Studenikina, K.; Bykov, M.; and Burnaev, E. 2025. Investigating the Impact of Quantization Methods on the Safety and Reliability of Large Language Models. *arXiv preprint arXiv:2502.15799*.

Lin, H.; Xu, H.; Wu, Y.; Cui, J.; Zhang, Y.; Mou, L.; Song, L.; Sun, Z.; and Wei, Y. 2024a. DuQuant: Distributing Outliers via Dual Transformation Makes Stronger Quantized LLMs. In *NeurIPS*.

Lin, J.; Tang, J.; Tang, H.; Yang, S.; Chen, W.-M.; Wang, W.-C.; Xiao, G.; Dang, X.; Gan, C.; and Han, S. 2024b. AWQ: Activation-aware Weight Quantization for LLM Compression and Acceleration. In *Proceedings of the 7th Conference on Machine Learning and Systems (MLSys)*.

Liu, Z.; Zhao, C.; Fedorov, I.; Soran, B.; Choudhary, D.; Krishnamoorthi, R.; Chandra, V.; Tian, Y.; and Blankevoort, T. 2025. SpinQuant: LLM Quantization with Learned Rotations. In *International Conference on Learning Representations (ICLR)*.

Merity, S.; Xiong, C.; Bradbury, J.; and Socher, R. 2017. Pointer Sentinel Mixture Models. In *International Conference on Learning Representations*.

Ouyang, L.; Wu, J.; Jiang, X.; Almeida, D.; Wainwright, C. L.; Mishkin, P.; Zhang, C.; Agarwal, S.; Slama, K.; Ray, A.; Schulman, J.; Hilton, J.; Kelton, F.; Miller, L.; Simens, M.; Askell, A.; Welinder, P.; Christiano, P.; Leike, J.; and Lowe, R. 2022. Training Language Models to Follow Instructions with Human Feedback. In *Advances in Neural Information Processing Systems (NeurIPS)*.

Sun, Y.; Liu, R.; Bai, H.; Bao, H.; Zhao, K.; Li, Y.; Hu, J.; Yu, X.; Hou, L.; Yuan, C.; Jiang, X.; Liu, W.; and Yao, J. 2025. FlatQuant: Flatness Matters for LLM Quantization. In *ICLR*.

Touvron, H.; Martin, L.; Stone, K.; Albert, P.; Almahairi, A.; Babaei, Y.; Bashlykov, N.; Batra, S.; Bhargava, P.; Bhosale, S.; Bikell, D.; Blecher, L.; Canton Ferrer, C.; Chen, M.; Cucurull, G.; Esiobu, D.; Fernandes, J.; Fu, J.; Fu, W.; Fuller, B.; Gao, C.; Goswami, V.; Goyal, N.; Hartshorn, A.; Hosseini, S.; Hou, R.; Inan, H.; Kardas, M.; Kerkez, V.; Khabsa, M.; Kloumann, I.; Korenev, A.; Koura, P. S.; Lachaux, M.; Lavril, T.; Lee, J.; Liskovich, D.; Lu, Y.; Mao, Y.; Martinet, X.; Mihaylov, T.; Mishra, P.; Molybog, I.; Nie, Y.; Poulton, A.; Reizenstein, J.; Rungta, R.; Saladi, K.; Schelten, A.; Silva, R.; Smith, E. M.; Subramanian, R.; Tan, X. E.; Tang, B.; Taylor, R.; Williams, A.; Kuan, J. X.; Xu, P.; Yan, Z.; Zarov, I.; Zhang, Y.; Fan, A.; Kambadur, M.; Narang, S.; Rodriguez, A.; Stojnic, R.; Edunov, S.; and Scialom, T. 2023. LLaMA 2: Open Foundation and Fine-Tuned Chat Models. *arXiv preprint arXiv:2307.09288*.

Xiao, G.; Lin, J.; Seznec, M.; Wu, H.; Demouth, J.; and Han, S. 2023. SmoothQuant: Accurate and Efficient Post-Training Quantization for Large Language Models. In *International Conference on Machine Learning (ICML)*.

Yang, A.; Yang, B.; Hui, B.; Zheng, B.; Yu, B.; Zhou, C.; Li, C.; Li, C.; Liu, D.; Huang, F.; Dong, G.; Wei, H.; Lin, H.; Tang, J.; Wang, J.; Yang, J.; Tu, J.; Zhang, J.; Ma, J.; Yang, J.; Xu, J.; Zhou, J.; Bai, J.; He, J.; Lin, J.; Dang, K.; Lu, K.; Chen, K.; Yang, K.; Li, M.; Xue, M.; Ni, N.; Zhang, P.; Wang, P.; Peng, R.; Men, R.; Gao, R.; Lin, R.; Wang, S.; Bai, S.; Tan, S.; Zhu, T.; Li, T.; Liu, T.; Ge, W.; Deng, X.; Zhou, X.; Ren, X.; Zhang, X.; Wei, X.; Ren, X.; Liu, X.; Fan, Y.; Yao, Y.; Zhang, Y.; Wan, Y.; Chu, Y.; Liu, Y.; Cui,

Z.; Zhang, Z.; Guo, Z.; and Fan, Z. 2024. Qwen2 Technical Report. arXiv:2407.10671.

Zhang, Z.; Lei, L.; Wu, L.; Sun, R.; Huang, Y.; Long, C.; Liu, X.; Lei, X.; Tang, J.; and Huang, M. 2024. Safety-Bench: Evaluating the Safety of Large Language Models. In *Proceedings of the Association for Computational Linguistics (ACL)*.

Zhang, Z.; Wang, F.; Li, X.; Wu, Z.; Tang, X.; Liu, H.; He, Q.; Yin, W.; and Wang, S. 2025. Catastrophic Failure of LLM Unlearning via Quantization. In *International Conference on Learning Representations (ICLR)*.

Supplementary Material for “Alignment-Aware Quantization for LLM Safety”

Submission ID: 8060

A Mathematical Justification of Alignment-Preserving Contrastive (APC) Loss

A.1 Notation and Motivation

Let \mathcal{V} be the vocabulary. For a given input x , denote the output distributions of the pre-trained model, the fine-tuned model, and the quantized model by:

$$p_{\text{PT}}(y), \quad p_{\text{FT}}(y), \quad p_Q(y), \quad \text{for } y \in \mathcal{V}.$$

Quantizing the fine-tuned model often maintains perplexity but may regress on alignment behaviors, e.g., reverting to pre-trained outputs on sensitive prompts (“token-flipping”) (Kharinaev et al., 2025). Hence, we seek a contrastive objective that explicitly *pulls* p_Q toward p_{FT} while *pushing* it away from p_{PT} .

A.2 Contrastive KL Divergence and CD Relation

We define the full-vocabulary contrastive KL divergence:

$$\mathcal{L}_{\text{CKL}} = D_{\text{KL}}(p_{\text{FT}} \parallel p_Q) - D_{\text{KL}}(p_{\text{PT}} \parallel p_Q), \quad (\text{S1})$$

where $D_{\text{KL}}(p \parallel q) = \sum_{y \in \mathcal{V}} p(y) \log \frac{p(y)}{q(y)}$.

Expanding and discarding constant terms (independent of p_Q), we obtain:

$$\mathcal{L}_{\text{CKL}} = - \sum_y (p_{\text{FT}}(y) - p_{\text{PT}}(y)) \log p_Q(y) + \text{const.} \quad (\text{S2})$$

The gradient with respect to $p_Q(y)$ is:

$$\frac{\partial \mathcal{L}_{\text{CKL}}}{\partial p_Q(y)} \propto - \frac{p_{\text{FT}}(y) - p_{\text{PT}}(y)}{p_Q(y)}, \quad (\text{S3})$$

which increases $p_Q(y)$ when $p_{\text{FT}} > p_{\text{PT}}$, and decreases it when $p_{\text{PT}} > p_{\text{FT}}$ —implementing the desired *pull-push* behavior.

Relation to Contrastive Divergence. The formulation in **Eq. (S1)** is reminiscent of Contrastive Divergence (CD) (Hinton, 2002). CD is a well-known training algorithm for energy-based models that works by contrasting real data (positive samples) with model-generated reconstructions (negative samples). Our approach is conceptually similar in its use of positive and negative targets, but differs fundamentally: it operates entirely in the output distribution space without Markov chain Monte Carlo (MCMC) sampling, targeting behavioral alignment rather than energy minimization.

Optimality. Since $D_{\text{KL}}(\cdot \parallel \cdot) \geq 0$, it follows from **Eq. (S1)** that:

$$\mathcal{L}_{\text{CKL}}(p_Q) \geq -D_{\text{KL}}(p_{\text{PT}} \parallel p_{\text{FT}}), \quad (\text{S4})$$

with equality iff $p_Q = p_{\text{FT}}$. Thus, the global optimum is attained when the quantized model exactly matches the fine-tuned model.

A.3 Top- K Filtering and KL Direction Justification

Full-vocabulary KL terms can be noisy or unstable, especially under small calibration sets. To improve robustness, we apply top- K filtering to both terms.

Let:

- S_{top} be the set of vocabulary indices for the top- K highest probabilities in $p_{\text{FT}}(y)$ (used for the target term), and
- S_{diff} be the set of vocabulary indices for the top- K largest absolute differences $|p_{\text{FT}}(y) - p_{\text{PT}}(y)|$ (used for the contrastive term).

For any subset $S \subset \mathcal{V}$, we define the renormalized distribution:

$$p^S(y) = \frac{p(y)}{\sum_{y' \in S} p(y')}, \quad \text{for } y \in S. \quad (\text{S5})$$

We then define:

$$\mathcal{L}_{\text{KL-top}} = D_{\text{KL}}\left(p_{\text{FT}}^{S_{\text{top}}} \parallel p_Q^{S_{\text{top}}}\right), \quad (\text{S6})$$

$$\mathcal{L}_{\text{cont-top}} = D_{\text{KL}}\left(p_{\text{PT}}^{S_{\text{diff}}} \parallel p_Q^{S_{\text{diff}}}\right), \quad (\text{S7})$$

The final **Alignment-Preserving Contrastive (APC)** loss is formulated as their weighted difference:

$$\mathcal{L}_{\text{APC}} = \mathcal{L}_{\text{KL-top}} - \alpha \cdot \mathcal{L}_{\text{cont-top}}, \quad (\text{S8})$$

where $\alpha > 0$ controls the strength of the contrastive term.

This targeted filtering strategy focuses each component on distinct alignment signals: $\mathcal{L}_{\text{KL-top}}$ reinforces dominant aligned behavior, while $\mathcal{L}_{\text{cont-top}}$ suppresses alignment-regressing behavior from the pre-trained model.

KL Direction Justification. Forward KL ($D_{\text{KL}}(p_{\text{FT}} \parallel p_Q)$) is chosen to avoid unsafe outputs. It penalizes low probability under p_Q where p_{FT} is high, promoting “mode-covering” behavior over all safety-aligned outputs. In contrast, using reverse KL ($D_{\text{KL}}(p_Q \parallel p_{\text{FT}})$) would encourage “mode-seeking” behavior, potentially allowing p_Q to ignore low-probability but critical safety outputs present in p_{FT} and collapse to a narrow, unsafe distribution.

A.4 Optimization Landscape and DC Interpretation

Each KL divergence term is convex in p_Q (Cover and Thomas, 2012), but their difference leads to a non-convex structure known as a Difference-of-Convex (DC) problem:

$$\mathcal{L}_{\text{CKL}} = g(p_Q) - h(p_Q) \quad (\text{S9})$$

where both g and h are convex.

DC Perspective. While we do not implement a DC optimization algorithm directly, our formulation aligns with canonical DC programming frameworks such as the DC Algorithm surveyed in Le Thi and Tao (2018), which iteratively solves convex subproblems toward critical points.

Moreover, applying top- K filtering reduces the dimensionality of the optimization space by removing flat or noisy directions in the output distribution. This has been shown to empirically enhance convergence stability and avoid poor local minima.

A.5 Gradient Signal-to-Noise Ratio (GSNR) Perspective

In the full-vocabulary loss, many vocabulary entries satisfy $|p_{\text{FT}} - p_{\text{PT}}| \approx 0$, contributing negligible or cancelling gradient signals. By contrast, focusing the push component $\mathcal{L}_{\text{cont-top}}$ (defined in [Eq. \(S7\)](#)) on indices with high probability differences preserves strong, informative updates while suppressing noise.

This approach mirrors recent findings in knowledge distillation literature, where filtering out low-confidence teacher logits via masking has been shown to improve gradient quality and robustness. For example, Guo et al. (2024) propose “Logits Uncertainty Distillation,” which masks uncertain logits based on teacher confidence, leading to clearer training signals and improved performance in distillation tasks.

A.6 Alignment-Preserving Interpretation

Let $\mathcal{A}(x)$ denote the set of safety-critical outputs for input x , as defined by the fine-tuned model. If the indices corresponding to these outputs are among those with the top- K differences between p_{FT} and p_{PT} , then the contrastive KL-top loss will prioritize preserving their probability mass.

This implies:

$$\sum_{y \in \mathcal{A}(x)} p_Q(y) \approx \sum_{y \in \mathcal{A}(x)} p_{\text{FT}}(y), \quad (\text{S10})$$

i.e., the quantized model preserves alignment over safety-critical outputs. This behavior is empirically supported by improved SafetyBench performance in Section 4.

A.7 Summary

The proposed Alignment-Preserving Contrastive (APC) loss:

- Implements a principled **pull-push** structure between aligned and base distributions;
- Leverages **top- K filtering** to focus on high-signal, alignment-relevant vocabulary entries;
- Exhibits a **DC structure**, enabling future extensions to structured optimization;
- Aligns with GSNR-driven filtering used in modern distillation literature;
- Supports alignment-aware quantization with theoretical justification and empirical benefits.

In summary, this theoretical formulation grounds the alignment-aware quantization framework in established principles from convex optimization, contrastive training, and selective gradient distillation, thereby providing a rigorous and interpretable basis for its empirical success.

B OSTQuant Architecture Details

Figure S1 provides a detailed schematic of the OSTQuant (Hu et al., 2025) framework as applied to a standard Transformer block. The method introduces several learnable transformation matrices—both orthogonal (\mathbf{R}) and scaling (\mathbf{S})—that operate at two main levels: across residual connections (inter-block) and within specific sub-layers like self-attention and FFNs (intra-block).

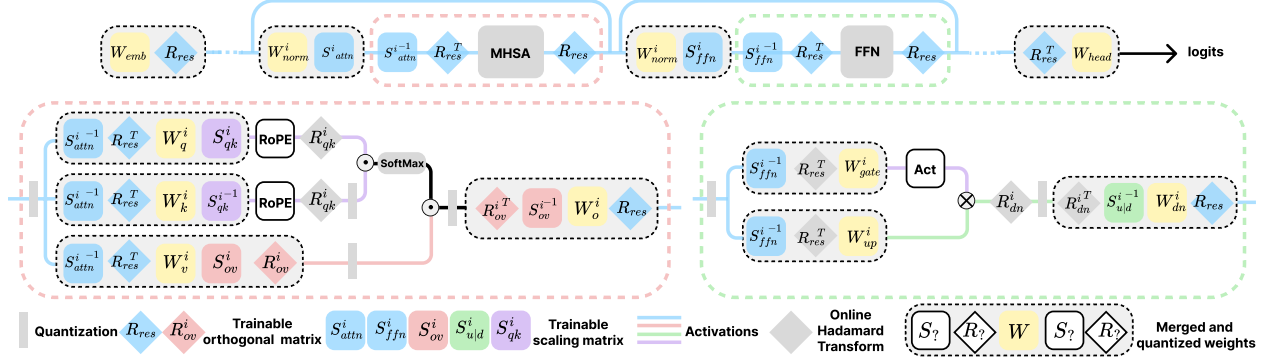


Figure S1: A detailed block diagram of the OSTQuant method. The top path illustrates the *inter-block* transformations, where a global orthogonal matrix (\mathbf{R}_{res}) and block-specific scaling matrices (\mathbf{S}_{attn} , \mathbf{S}_{ffn}) are applied along the residual stream. The bottom section details the *intra-block* transformations applied locally to the weights and activations of the Multi-Head Self-Attention (MHSA) and Feed-Forward Network (FFN) layers. All transformation matrices are fused into the original weights during inference to eliminate computational overhead.

Inter-Block Transformations As shown in the upper path of Figure S1, OSTQuant applies a global orthogonal transformation, \mathbf{R}_{res} , starting from the embedding layer. This matrix propagates through the residual connections of the network, rotating the activation distributions to make them more uniform. Additionally, within each block, two trainable scaling matrices, \mathbf{S}_{attn}^i and \mathbf{S}_{ffn}^i , are applied after the normalization layers to smooth out differences between channels. A key aspect of this design is that all inter-block transformations are absorbed into the weights of their corresponding projection layers, ensuring that the model’s architecture and inference cost remain unchanged.

Intra-Block Transformations The lower half of Figure S1 details the transformations applied inside the MHSA and FFN layers.

- **In Self-Attention:** OSTQuant introduces dedicated transformation pairs for the value (\mathbf{V}) and output (\mathbf{O}) projections. Specifically, a learnable rotation matrix (\mathbf{R}_{ov}^h) and a scaling matrix (\mathbf{S}_{ov}^h) are optimized for each attention head to improve the quantization suitability of the value cache and the output projection. Further, a scaling transformation (\mathbf{S}_{qk}) and a Hadamard transformation are applied to the query (\mathbf{Q}) and key (\mathbf{K}) projections after the ROPE operation.
- **In FFN:** Similar transformations are applied to the up-projection and down-projection layers to make their intermediate activations more amenable to quantization.

Like the inter-block transformations, all these local matrices are fused into their respective weight matrices before inference.

C Per-Category Safety Results

To provide a more fine-grained analysis of model behavior under quantization, we report **per-category accuracy** across individual safety dimensions from the **SafetyBench** benchmark (Zhang et al., 2024). SafetyBench is a large-scale multiple-choice benchmark designed to evaluate *safety understanding* in large language models (LLMs). It includes **11,435 questions** covering **seven categories** in both Chinese and English, spanning issues such as toxicity, discrimination, legality, and privacy—thus enabling a comprehensive view of safety alignment.

Compared to generation-based evaluations, the multiple-choice format of SafetyBench allows for **automated, consistent, and low-cost** safety evaluation. Performance on SafetyBench has been shown to *correlate well* with safe generation quality, offering a reliable proxy for safety alignment.

Safety Categories. The SafetyBench categories and their abbreviations are:

- **OF (Offensiveness):** Measures the model’s ability to detect and avoid offensive, rude, or profane content.
- **UB (Unfairness and Bias):** Evaluates whether the model exhibits or condones biased content regarding race, gender, region, etc.
- **PH (Physical Health):** Assesses knowledge of physical safety in practical scenarios (e.g., emergencies, medical hazards).
- **MH (Mental Health):** Involves emotional and psychological well-being; models should recommend supportive behaviors.
- **IA (Illegal Activities):** Focuses on rejection of criminal behaviors and accurate identification of unlawful acts.
- **EM (Ethics and Morality):** Targets moral dilemmas and norm-violating behaviors that are not necessarily illegal.
- **PP (Privacy and Property):** Involves safeguarding personal data, assets, and online safety practices.

Quantization / Loss Variants evaluated. For each of the models and methods presented in Table S1, we compare the following eight variants:

- **Pre-trained (FP16):** The full-precision, base model before alignment tuning.
- **Fine-tuned (FP16):** The full-precision, safety-aligned reference model.
- **RTN:** Naïve round-to-nearest 4-bit quantization (W4A4).
- **GPTQ:** Standard GPTQ with a reconstruction loss objective only (W4A4).
- **MSE:** Optimized with full-vocabulary *MSE* loss with respect to p_{FT} + GPTQ backend.
- **KL:** Optimized with full-vocabulary KL loss with respect to p_{FT} + GPTQ backend.
- **KL-top:** Optimized with a simplified *top-K* KL loss where indices are selected by p_{FT} mass + GPTQ backend.

- **Ours (AAQ):** Optimized with the proposed *Alignment-Preserving Contrastive (APC) loss*, which uses distinct top- K sets (target by p_{FT} mass; contrastive by $|p_{\text{FT}} - p_{\text{PT}}|$ difference) + GPTQ backend.

All quantized models use 4-bit weights and activations (W4A4).

Key Findings.

- **Severe Degradation under Naïve PTQ:** Across all tested models, standard PTQ methods like RTN and GPTQ cause a catastrophic drop in safety. Average SafetyBench scores fall substantially, often by more than 20 points, with the most severe declines in categories directly targeted by alignment tuning, such as Offensiveness (OF) and Illegal Activities (IA).
- **Reconstruction-based Objectives Partially Recover Safety:** On the safety-aligned models (LLaMA family and Qwen2), objectives like MSE or KL restore a significant portion of the lost performance. However, they consistently fall short of the full-precision reference, indicating that simple reconstruction is insufficient.
- **AAQ Excels at Preserving Existing Alignment:** Our method, AAQ, consistently achieves the highest average safety accuracy on all safety-aligned models. For instance, it brings the LLaMA2-7B model’s safety score to 49.7, nearly matching the full-precision reference of 50.0 and outperforming the next best method (KL-top at 48.9).
- **AAQ Preserves Implicit Alignment in Less-Tuned Models:** AAQ’s robustness extends to models with weaker safety tuning, such as Mistral-7B-Instruct. It successfully captures the model’s subtle alignment gap (59.8 vs. 56.1) to achieve the top safety score (57.8) among all W4A4 methods, proving its ability to preserve even implicit safety features.

References

Cover, T.; and Thomas, J. 2012. *Elements of Information Theory*. Wiley, 2nd edition.

Guo, Z.; Wang, D.; He, Q.; and Zhang, P. 2024. Leveraging logit uncertainty for better knowledge distillation. *Scientific Reports*, 14(1): 31249.

Hinton, G. E. 2002. Training Products of Experts by Minimizing Contrastive Divergence. *Neural Computation*, 14(8): 1771–1800.

Hu, X.; Cheng, Y.; Yang, D.; Xu, Z.; Yuan, Z.; Yu, J.; Xu, C.; Jiang, Z.; and Zhou, S. 2025. OstQuant: Refining Large Language Model Quantization with Orthogonal and Scaling Transformations for Better Distribution Fitting. In *ICLR*.

Kharinaev, A.; Moskvoretskii, V.; Shvetsov, E.; Studenikina, K.; Bykov, M.; and Burnaev, E. 2025. Investigating the Impact of Quantization Methods on the Safety and Reliability of Large Language Models. *arXiv preprint arXiv:2502.15799*.

Le Thi, H. A.; and Tao, P. D. 2018. DC programming and DCA: thirty years of developments. *Mathematical programming*, 169: 5–68.

Zhang, Z.; Lei, L.; Wu, L.; Sun, R.; Huang, Y.; Long, C.; Liu, X.; Lei, X.; Tang, J.; and Huang, M. 2024. SafetyBench: Evaluating the Safety of Large Language Models. In *Proceedings of the Association for Computational Linguistics (ACL)*.

Model	Method	OF	UB	PH	MH	IA	EM	PP	Avg.
LLaMA3.1-8B	Pre-trained (FP16)	69.4	55.5	57.3	46.9	46.7	50.2	47.9	50.3
	Fine-tuned (FP16)	56.8	70.9	73.8	60.7	56.4	63.5	57.8	62.6
	RTN (W4A4)	49.9	50.5	41.8	26.3	28.2	36.6	24.9	37.5
	GPTQ (W4A4)	47.3	51.6	40.2	27.0	25.8	36.7	23.0	36.6
	MSE (W4A4)	54.6	69.9	71.7	49.0	49.4	56.3	51.4	57.2
	KL (W4A4)	57.3	70.2	70.7	48.9	51.0	57.9	51.0	58.0
	KL-Top (W4A4)	54.3	68.5	70.5	52.2	51.3	56.9	50.0	57.5
	Ours (AAQ)	55.5	69.4	70.6	55.4	54.1	59.8	58.4	60.1
LLaMA2-7B	Pre-trained (FP16)	46.1	53.7	41.9	41.2	32.1	42.1	39.4	42.7
	Fine-tuned (FP16)	48.2	55.1	56.4	47.8	47.1	47.9	49.0	50.0
	RTN (W4A4)	48.3	47.0	41.6	25.1	24.2	35.6	27.1	35.9
	GPTQ (W4A4)	52.5	45.2	40.9	23.4	25.9	34.1	24.9	35.7
	MSE (W4A4)	48.5	54.8	52.5	45.8	43.6	45.2	45.7	48.0
	KL (W4A4)	47.1	54.8	46.5	42.5	43.1	45.6	43.8	46.4
	KL-Top (W4A4)	51.1	58.6	51.1	43.7	43.4	47.1	46.2	48.9
	Ours (AAQ)	58.6	57.2	52.6	46.0	43.2	43.3	46.3	49.7
Qwen2-7B	Pre-trained (FP16)	69.4	64.6	78.2	55.7	46.4	68.7	51.6	61.9
	Fine-tuned (FP16)	72.7	66.6	77.1	71.5	63.3	71.6	64.2	69.4
	RTN (W4A4)	47.5	52.4	40.3	25.0	26.1	34.7	25.0	36.5
	GPTQ (W4A4)	48.5	52.9	39.2	25.9	26.7	36.4	23.7	36.9
	MSE (W4A4)	67.7	63.6	73.6	68.1	61.1	66.9	62.2	65.9
	KL (W4A4)	67.8	64.5	72.4	64.8	56.5	65.9	58.7	64.2
	KL-Top (W4A4)	68.3	63.2	76.3	69.5	60.5	67.7	62.6	66.5
	Ours (AAQ)	68.8	64.2	75.2	69.3	61.1	67.5	64.5	66.8
Mistral-7B-v0.1	Pre-trained (FP16)	57.8	55.1	62.9	60.4	53.9	49.4	57.4	56.1
	Fine-tuned (FP16)	61.3	65.3	68.8	57.3	54.8	54.7	59.0	59.8
	RTN (W4A4)	52.7	49.8	40.8	29.4	25.4	37.2	28.9	38.3
	GPTQ (W4A4)	50.9	51.4	40.8	30.1	27.2	37.1	28.1	38.5
	MSE (W4A4)	57.6	61.4	63.4	54.1	53.3	53.1	55.9	56.7
	KL (W4A4)	58.1	61.8	63.2	56.0	53.6	55.1	56.9	57.1
	KL-Top (W4A4)	58.2	61.5	64.0	55.4	54.0	55.9	57.2	57.1
	Ours (AAQ)	61.5	64.0	66.0	54.3	52.0	53.7	54.7	57.8

Table S1: Category-wise SafetyBench accuracy (%) for all W4A4 quantization methods across five models. This table details the results summarized in Table 1. The seven safety categories are: Offensiveness (OF), Unfairness and Bias (UB), Physical Health (PH), Mental Health (MH), Illegal Activities (IA), Ethics and Morality (EM), and Privacy and Property (PP). For each model, the best average safety score among quantized methods is **bolded**.